Combustion and Flame 220 (2020) 16–22

Contents lists available at ScienceDirect

Combustion and Flame

journal homepage: www.elsevier.com/locate/combustflame

Dependence of kinetic sensitivity direction in premixed flames

Weiqi Ji [a], Tianwei Yang [b], Zhuyin Ren [b], Sili Deng [a,*]

[a] Department of Mechanical Engineering, Massachusetts Institute of Technology, MA 02139, USA
[b] Center for Combustion Energy, Tsinghua University, Beijing 100084, China

ARTICLE INFO

Article history:
Received 12 April 2020
Revised 17 June 2020
Accepted 17 June 2020

Keywords:
Sensitivity Analysis
Uncertainty quantification
Sensitivity direction
Flamelet
Extinction strain rate

ABSTRACT

The sensitivities of turbulent combustion simulations to chemical kinetic parameters can be analyzed to understand the controlling reactions in turbulent flames and to quantify the uncertainties in simulations. However, computing the sensitivity of turbulent combustion simulations to a large number of kinetic parameters is still challenging. A promising approach is to estimate the sensitivity from laminar flames, especially for cases where the flamelet model is applicable. Under these conditions, the underlying hypothesis is that the sensitivity direction of the flamelet profiles is independent of the strain rate and the flame coordinate, which is the progress variable for premixed flames. In the present work, this hypothesis was tested in laminar premixed counterflow flames. We first studied the sensitivity directions of two extreme cases, the near-extinction strained flames and the freely propagating unstretched flames. It was found that the sensitivity directions of the extinction strain rate and the laminar flame speed are aligned with each other for various fuels, equivalence ratios, and pressures. We then studied the dependence of the sensitivity direction of the maximum flame temperature on the strain rate as well as the dependence of the sensitivity direction of the species profiles on the progress variable. It was found that the sensitivity direction of maximum temperature was largely independent of the strain rate. Moreover, the sensitivity directions of the temperature and species profiles were independent of the progress variable, and they were all similar to the sensitivity direction of the extinction strain rate. These findings suggest that there is a universal sensitivity direction for turbulent premixed flames and the direction can be estimated by the sensitivity direction of extinction strain rate. These conclusions will enable efficient sensitivity analysis of turbulent combustion simulations when the hypothesis is valid.

1. Introduction

In order to accurately capture the pollution formation processes, modern turbulent combustion simulations usually adopt detailed chemical models which contain thousands of species and reactions. Since reaction rates are inevitably associated with certain uncertainties, it is often desirable to quantify the influence of the uncertainties in the chemical kinetic parameters on the simulation and to understand what reactions dominant the uncertainty [1–4].

A common approach to elucidate the kinetic uncertainty is to conduct sensitivity analysis, such that the linear response of the flame profiles to small perturbations of the kinetic parameters is quantified [5–7]. The uncertainty can also be estimated by first-order Taylor expansion with the sensitivity as the derivative [8]. Due to the high computational cost of turbulent combustion simulations, conducting sensitivity analysis for a large number of kinetic parameters is impractical.

A potential approach to estimate the kinetic sensitivity of the expensive turbulent combustion simulations is to relate the sensitivity to that of the less expensive laminar flames. For example, Mueller et al. [1] proposed to estimate the uncertainties of flamelet-based large eddy simulations based on the uncertainties of steady flamelets. Although not explicitly mentioned by Mueller et al. [1], the underlying hypothesis for the estimation is that the sensitivity directions of the flamelet profiles under different strain rates and flame coordinates (the mixture fraction for non-premixed flames and progress variable for premixed flames) are the same. In other words, flamelet profiles under different strain rates and flame coordinates will change simultaneously with the perturbation of the kinetic parameters. For example, the changes of the temperature at two different strain rates but same flame coordinates upon kinetic perturbation will be proportional to each other. Therefore, the uncertainty of the flamelet can be parameterized by a single variable along the unified sensitivity direction, such that the high-dimensional kinetic uncertainty is reduced

* Corresponding author.
E-mail address: silideng@mit.edu (S. Deng).

https://doi.org/10.1016/j.combustflame.2020.06.027
0010-2180/

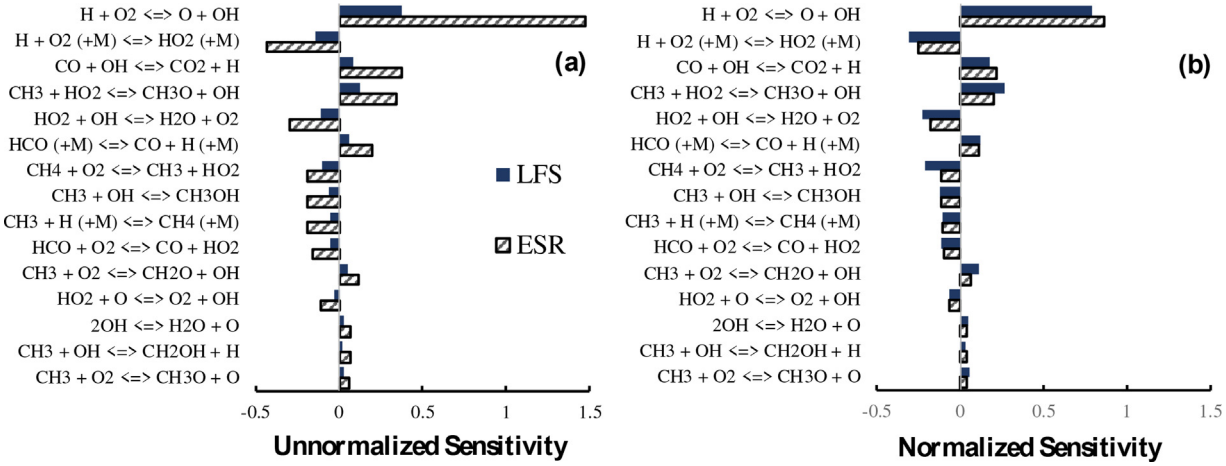

Fig. 1. Sensitivity analysis of LFS and ESR of the methane/air mixture with an equivalence ratio of 0.7 and at 30 atm using a detailed mechanism [14]. (a) Unnormalized sensitivities, (b) Normalized sensitivities.

to one-dimensional uncertainty. Furthermore, the entire turbulent flame share the same sensitivity direction everywhere, although the flame involves a wide range of strain rates and mixture fractions/progress variables. Similarly, the universal sensitivity direction assumption is also required for the estimation of the active subspace of turbulent flames based on laminar flames [3].

However, the hypothesis has not been validated in the literature since the sensitivity analysis of turbulent flames is only available recently. Therefore, this work aims to test this hypothesis in laminar premixed flames and build theoretical foundations for developing efficient algorithms for the sensitivity analysis of turbulent combustion simulations. We shall first study the sensitivity directions of two extreme cases of near-extinction strained flames and freely propagating unstretched flames. We will then study the dependence of the sensitivity direction of the maximum flame temperature on the strain rate and that of the species profiles on the progress variable.

2. Sensitivity directions of extinction strain rate and laminar flame speed

Laminar freely propagating flames and counterflow flames near the extinction point are two extreme cases of strained flames. They are usually characterized by the laminar flame speed (LFS) and the extinction strain rate (ESR), respectively. Therefore, we first study the sensitivity directions of ESR and LFS to investigate the effect of strain on the sensitivity directions. Since LFS is much more extensively studied than ESR both experimentally and numerically, we herein only briefly discuss about the computation of ESR and its sensitivity directions.

The ESR characterizes the response of the flame to strain. A higher ESR indicates that the mixture is more likely to sustain combustion in strained flows. ESR is usually measured and simulated in premixed counterflow twin flames, the response of which can be described via the S-curve analysis [9]. The maximum strain rate that the flame can sustain with fixed composition and thermodynamic states at the inlet is defined as the ESR. Specifically, the absolute value of the maximum velocity gradient is often utilized to evaluate ESR. Numerically, since the ESR corresponds to a singularity point, it has to be solved using either flame continuation approach [10] or reducing factor approach [11].

The continuation approach enables an efficient sensitivity analysis of the ESR as first proposed in [12]. By realizing that ESR becomes a dependent variable when the two-point continuation approach [10] is invoked, it is possible to perform rigorous sensitivity analysis with respect to kinetic rate constants for ESR at the exact strain rate determined experimentally. In the reducing factor approach, the simulation of the counterflow premixed flame starts from a low strain rate and gradually increases to the near-extinction state. The step size of the increment of the strain rate should be gradually decreased to retain the burning solutions up to the extinction point. Such an approach has been implemented in the open-source software of Ember [11], and the reducing factor approach with Ember has been reported to be more efficient than the continuation approach implemented in Chemkin [13]. However, the sensitivity of ESR has to be evaluated using the finite difference method in the reducing factor approach, which could be computationally expensive. Nonetheless, in both approaches, the sensitivity is usually reported in its dimensionless form,

$$s_i = \frac{\partial ln[ESR]}{\partial ln[k_i]} = \frac{k_i}{ESR}\frac{\partial [ESR]}{\partial [k_i]}, \tag{1}$$

where k_i is the rate constant for the i th reaction, and s_i is the corresponding sensitivity coefficient. The sensitivity coefficients for all reactions can be stacked into a sensitivity vector, i.e., $\mathbf{S} = [s_1, s_2, \ldots, s_n]$. Furthermore, the sensitivity vector is normalized by its magnitude $||\mathbf{S}||_2$ to obtain the sensitivity direction $\tilde{\mathbf{S}}$ ($\tilde{\mathbf{S}} = \mathbf{S}/||\mathbf{S}||_2$). Therefore, the sensitivity direction represents the normalized sensitivities of all reactions.

Figure 1 shows the sensitivity analysis of LFS and ESR of a methane/air mixture using the detailed mechanism in Hashemi et al. [14]. The equivalence ratio is 0.7, and the pressure is 30 atm, which are kept the same as Long et al. [15]. The unnormalized and normalized sensitivities are shown in Figs. 1a and 1b, respectively. It can be seen that the sensitivity rankings for ESR and LFS are almost the same, with the most sensitive reaction being the primary chain-branching reaction of H + O_2<=>O+OH. The observation is consistent with many existing studies [15–17] which pointed out that the ESR and the LFS share the same set of controlling reactions. Overall, the magnitude of the sensitivity of ESR is larger than that of LFS. As pointed out in [15], this result is consistent with previous studies that showed LFS to scale with the square root of the overall reaction rate [18] while ESR was shown to scale linearly [19]. Therefore, normalization of the sensitivity by the sensitivity magnitude is necessary to assess the relative sensitivity of different reactions. Surprisingly, the normalized sensitivity for ESR and LFS are very similar to each other as shown in Fig. 1b. We consequently denote the alignment of the sensitivity directions as the kinetic similarity.

Table 1
The kinetic similarity between ESR and LFS evaluated for the sensitivities in the literature.

No.	Fuel	Phi	Cosine	Top N	p[atm]	Ref.	Alias
1	methanol	0.77	1.00	16	1	[27]	Holley2006
2	*iso*octane	0.87	0.46	12	1	[27]	Holley2006
3	*n*-dodecane	1.0	0.94	10	1	[24]	Kumar2007
4	*n*-dodecane	1.0	0.97	10	1	[24]	Kumar2007
5	*n*-dodecane	1.0	0.95	10	1	[24]	Kumar2007
6	dimethyl ether	0.6	1.00	10	1	[28]	Wang2009
7	dimethyl ether	1.0	0.99	10	1	[28]	Wang2009
8	dimethyl ether	1.5	0.91	10	1	[28]	Wang2009
9	*n*-butanol	0.6	0.59	8	1	[26]	Veloo2010
10	*n*-butanol	1.0	0.89	8	1	[26]	Veloo2010
11	*n*-butanol	1.5	0.96	8	1	[26]	Veloo2010
12	*n*-butanol	0.6	0.95	8	1	[26]	Veloo2010
13	*n*-butanol	1.0	0.97	8	1	[26]	Veloo2010
14	*n*-butanol	1.5	0.97	8	1	[26]	Veloo2010
15	*n*-dodecane	0.7	0.96	10	1	[16]	Ji2010
16	*n*-dodecane	1.0	0.97	10	1	[16]	Ji2010
17	*n*-dodecane	1.4	0.97	10	1	[16]	Ji2010
18	*n*-dodecane	1.0	0.95	12	1	[29]	Kumar2010
19	*n*-dodecane	1.0	0.97	10	1	[29]	Kumar2010
20	methyl-butanoate	0.7	0.97	14	1	[30]	Wang2011
21	methyl-butanoate	1.0	0.98	14	1	[30]	Wang2011
22	methyl-butanoate	1.5	0.97	14	1	[30]	Wang2011
23	*n*-propylbenzene	1.0	0.96	10	1	[31]	Hui2012
24	methane/C_2HF_5	1.0	0.96	14	1	[32]	Xu2017
25	methane/$C_2HF_3Cl_2$	1.0	0.99	14	1	[32]	Xu2017
26	methane/$C_3H_2F_3Br$	1.0	0.97	14	1	[32]	Xu2017
27	methane	0.7	0.98	15	1	[15]	Long2019
28	methane	0.7	0.99	15	7	[15]	Long2019
29	methane	0.7	0.98	15	30	[15]	Long2019
30	methane	1.3	0.99	15	1	[15]	Long2019
31	methane	1.3	0.97	15	7	[15]	Long2019
32	methane	1.3	0.98	15	30	[15]	Long2019

To measure the kinetic similarity between two sensitivity directions, the inner product between two normalized sensitivity vectors can be quantified, which is also termed as the cosine similarity [20–23]. The cosine similarity of unity corresponds to a perfect parallel, while zero indicates that two directions are orthogonal to each other. For the normalized sensitivities in Fig. 1b, the cosine similarity $\langle \tilde{\boldsymbol{S}}_{ESR}, \tilde{\boldsymbol{S}}_{LFS} \rangle$ is 0.98, which suggests that the two sensitivity directions are almost parallel. This result implies that the ESR and the LFS for the specified mechanism and conditions are kinetically similar, in the sense that they share not only the same set of controlling reactions but also the same response to the coupling among these reactions.

Next, we shall investigate the kinetic similarities between ESR and LFS with other fuels, equivalence ratios, and pressures. Computing the sensitivity of ESR for large hydrocarbon fuels could be time consuming since computing the ESR itself for large reaction model is already intensive [11] and hyperparameter tuning is often needed to save computational time while retaining a stable solution. Fortunately, the kinetic sensitivities of ESR are usually reported in the literature in addition to the experimental measurement of ESR. Therefore, we compiled the sensitivity analysis results of ESR as well as those of LFS from literature and normalized the sensitivities to obtain the cosine similarity.

The compiled database is summarized in Table 1. The investigated conditions cover a wide variety of fuel, equivalence ratios (phi), and pressures (p [atm]). The “top N” in the table refers to the number of top-ranked sensitive reactions presented in the literature. For most of the cases, the cosine similarity is higher than 0.95, which suggests that the two sensitivity directions for ESR and LFS are very similar to each other. The consistency between large hydrocarbon fuels and methane agrees with previous studies [16,17,24] which suggest that the ESR is most sensitive to small-molecule reactions, i.e., $H_2/CO/C_1–C_2$ kinetics.

Note that there are a few outliers that have noticeable lower cosine similarity than the others. Regarding the outliers of #9–10, the difference is potentially because the ESR at lean condition is insensitive to the reaction of CO+OH<=>CO_2+H with the kinetic model published in 2009 [25]. The model significantly underpredicted the ESR for lean and stoichiometric conditions. The predictions with the updated model employed in [26] agreed much better with the experimental data. Correspondingly, the difference in the sensitivity direction is significantly reduced, as shown in #12–13. For the dataset of #2, the cause of the difference is suspected to be that the ESR is extremely sensitive to C_3H_4+O<=>CH_2O+C_2H_2 based on the kinetic model published in 1998 [12]. The model showed large discrepancies from the experimental data of ESR. Therefore, it can be summarized that the similarity between the kinetic sensitivity of ESR and LFS is an inherent property of fuel-air mixtures, although such similarity might not show in computations if the models significantly off predict the experimental measurements.

It is worth to mention that the kinetic similarity is consistent with the historical views on the connection between ESR and LFS based on the time scale analysis by Peters [33]. The flame residence time in flame propagation is given by the ratio between the flame thickness and LFS, while the quench time for flame extinction is given by the inverse of ESR. The numerical simulations by Rogg [34] for a stoichiometric methane-air flame show that the flame residence time and the quench time are very close to each other, such that the quench time is subsequently approximated by the flame residence time in flame propagation for turbulent combustion modeling. Since both time scales are equal to the chemical time scale [33], one can imply that flame extinction has similar chemical time scale with the unstretched flame propagation. Since the chemical time scale is determined by the controlling reactions, the similarity of the controlling reactions and the sensitivity directions is consistent with the similarity in the time scales. It is

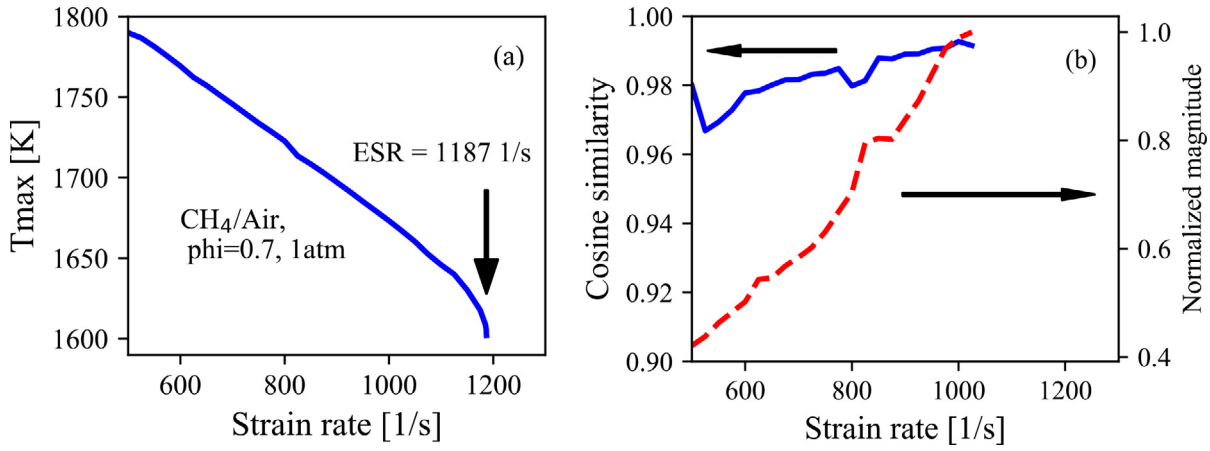

Fig. 2. (a) The response of the maximum flame temperature versus the strain rate. (b) The evolution of the cosine similarity and normalized magnitude with strain rates. The sensitivity magnitude is normalized by the maximum magnitude at the strain rate of 1075 1/s. The cosine similarity refers to the inner product between the sensitivity direction at each strain rate and the sensitivity direction of ESR.

worthy to note that the above time scale analysis is qualitative, since the chemical time scale of LFS is not always equal to that of ESR [19], and the flame temperature at extinction is much lower than the unstretched flame. Thus, the classical time analysis cannot fully explain the quantitative similarity of the sensitivity directions. Therefore, more rigorous analysis on the dependence of sensitivity directions on the strain rate and flame temperature will be carried out in Section 3.

Leveraging the kinetic similarity between ESR and LFS, the sensitivity of ESR can be efficiently computed based on the sensitivity of LFS. Specifically, the similarity implies that

$$\frac{\partial \ln[ESR]}{\partial \ln[k_i]} \Big/ \frac{\partial \ln[ESR]}{\partial \ln[k_m]} = \frac{\partial \ln[LFS]}{\partial \ln[k_i]} \Big/ \frac{\partial \ln[LFS]}{\partial \ln[k_m]}, \tag{2}$$

where the sensitivity of LFS to all reactions can be efficiently computed with the adjoint approach. Therefore, to evaluate the sensitivity coefficients of ESR for all reactions, we just need to compute the sensitivity of ESR to the most sensitive reaction k_m via the finite difference approach, and sensitivities to other reactions are readily available via Eq. (2). The efficient computation of the sensitivity of ESR will benefit the gradient-based optimization and uncertainty quantification for ESR [35].

3. Dependence of sensitivity direction on strain rate and progress variable

Next, we shall study the evolution of sensitivity directions of flame temperatures and species concentrations with the strain rate and the progress variable. The sensitivities of the flame temperature and species concentrations are also computed using Ember with the finite difference approach for the top 15 reactions preselected based on the sensitivity of LFS. The simulation is conducted for a methane/air mixture using the detailed mechanism of GRI3.0 [36]. Details on the composition and thermodynamic states are: equivalence ratio of 0.7, inlet temperatures of 300 K, and atmospheric pressure.

Figure 2a shows the response of the maximum temperature with the strain rate in the upper branch of the S-curve, and the ESR is around 1187 1/s. Since the perturbation of the kinetic rate constants also affects the ESR, the temperature and species sensitivity are computed from the strain rate of 500 to 1075 1/s. Figure 2b then shows the evolution of the sensitivity vector of the maximum temperature T_{max} with strain rates. The sensitivity magnitude is normalized by the maximum magnitude at the strain rate of 1075 1/s. In order to display the sensitivity directions at all strain rates examined, we compute their cosine similarity with a reference sensitivity direction, which is that of the ESR. As expected, the sensitivity magnitude increases with the strain rate since the flame is more sensitive to chemical kinetics when approaching extinction.

Moreover, the sensitivity directions of T_{max} are independent of the strain rate, and they are similar to the sensitivity direction of ESR with the minimum cosine similarity of 0.97 for the specified range of strain rates. Therefore, the controlling reactions of T_{max} are independent with the strain rate. The independence is intriguing since the peak temperature, local chemical time scale, and sensitivity magnitude of the flame all vary with strain rate. The independence also explain why the ESR and LFS share the same sensitivity direction while the local chemical time scales could be different for ESR and LFS [19].

The evolution of the sensitivity directions of flame temperatures and species concentrations with the locations in the flame coordinate is further investigated to examine if there is a universal kinetic sensitivity direction for premixed flames. Figure 3a presents the temperature profile as a function of the distance to the stagnation-point. The perturbed profiles correspond to the solutions with perturbed rate constants. The gap between the original and perturbed profiles indicates the magnitude of sensitivity. It can be seen that the sensitivity magnitude is substantial near the flame front, which corresponds to a large temperature gradient. The evolution of the sensitivity magnitudes is further detailed in Fig. 3b. The magnitude is normalized by the maximum magnitude in the entire flame domain. The magnitude of the sensitivity is much weakened in the cold unburned regime and the hot equilibrium regime. Figure 3b also shows the evolution of the sensitivity direction, where the cosine similarity is computed with respect to the sensitivity direction of ESR. The evolution of the cosine similarity suggests that the sensitivity directions are almost the same across the entire flame and are the same as that of ESR. The cosine similarity is above 0.9 for most of the locations, and the sensitivity magnitude is negligible when the cosine similarity is below 0.9. In other words, a global similarity of the sensitivity direction is elucidated. Such global similarity has been previously observed in the homogenous auto-ignition system and one-dimensional burner stabilized flame [20–22].

To further elaborate the implications of the independence of sensitivity directions with locations in the flame coordinate, Fig. 3a presents the changes of temperature at two distinct locations x_1

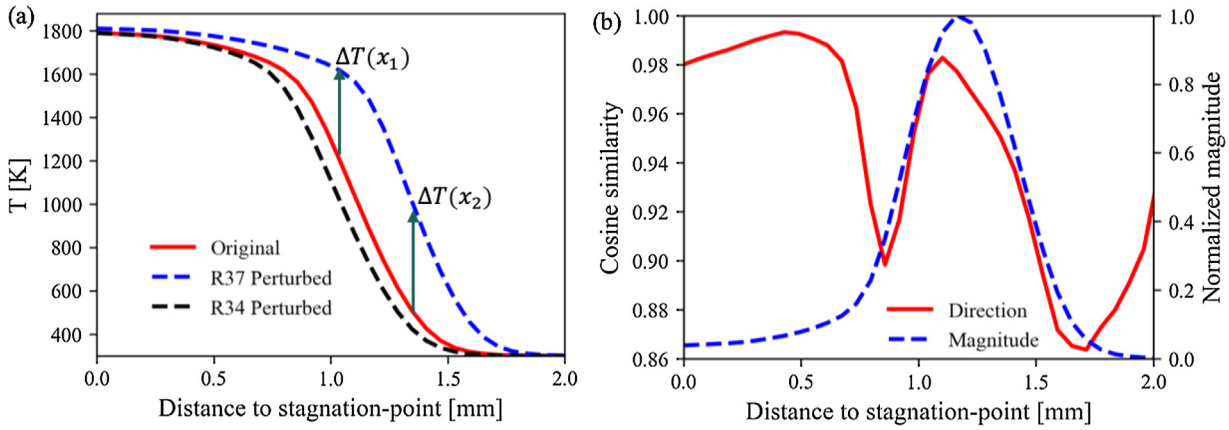

Fig. 3. (a) The temperature profiles of flames with unperturbed and perturbed reactions in the flame coordinate. (b) The evolution of the direction and magnitude of the temperature sensitivity with the distance to stagnation-point. The cosine similarity is computed with respect to the sensitivity direction of ESR. All results are computed under the strain rate of 500 1/s.

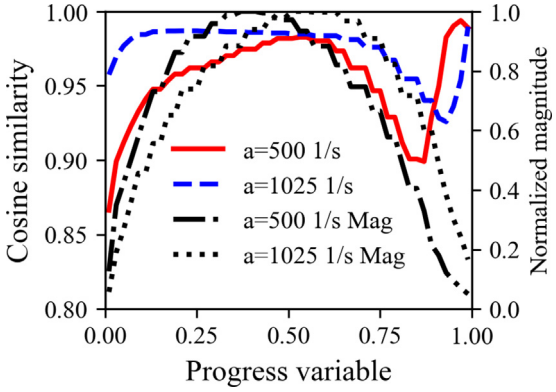

Fig. 4. The evolution of the direction and magnitude of sensitivity of the flame temperature with the progress variable and the strain rate. The cosine similarity is computed with respect to the sensitivity direction of ESR. The magnitude is normalized by the maximum magnitude across the entire flame domain at each strain rate.

and x_2. The independence implies that the ratio of the temperature changes $\Delta T(x_1)/\Delta T(x_2)$ is constant no matter what and how reaction rate constants are perturbed. The constant ratio will enable us to parameterize the uncertainties of the temperature profiles using a single random variable, which could potentially reduce the computational cost for uncertainty quantifications.

We then present the sensitivity in the progress variable space for clear visualization since the compositions could change sharply in the narrow reaction zone. The progress variable c is defined in terms of the temperature, i.e.,

$$c = \frac{T - T_{\min}}{T_{\max}(a) - T_{\min}}, \tag{3}$$

where the maximum temperature $T_{\max}$ changes with the strain rate a. The progress variable c is within the range of [0, 1]. The minimum temperature $T_{\min}$ is the inlet temperature of 300 K. Figure 4 shows the evolution of sensitivity directions of the flame temperature with progress variable at two representative strain rates. It again can be shown that the cosine similarity with ESR is higher than 0.9 in most of the high-temperature regime. It is noted that the cosine similarity deviates from unity when the progress variable is close to zero or is between 0.7 and 0.9. However, it is found that the magnitude of the sensitivity drastically reduces in the region where the cosine similarity deviates from unity, indicating that the local temperature is not sensitive to the kinetic parameters. In addition, the cosine similarity recovers to unity in the reaction zone, i.e., near $c = 1$. Therefore, evaluating the overall similarity across the progress variable based on the global sensitivity direction is still valid. Furthermore, the sensitivity direction of the flame temperature is also approximately independent of the strain rate by comparing the evolutions at two distinct strain rates. These observations suggest that the temperature sensitivity direction keeps the same across the flame in the flow with various degrees of strain. Intuitively, the temperature sensitivity is a result of the sensitivity of heat release rate, and the changes of the flame temperature due to flame stretch do not alter the controlling reactions for heat release.

Next, the evolution of the sensitivity direction of the species mass fractions with progress variable and strain rate are also studied for their relevance to emissions, as shown in Fig. 5. The sensitivity directions for major species, CH_4 and CO (Figs. 5a and 5b, respectively), are also largely independent of the progress variable and are similar to the sensitivity direction of ESR. The sharp switching between positive and negative correlations corresponds to the local maximum species concentration [20]. The progress variable corresponding to the local maximum species concentration divides the flame into two kinetic regimes. Take Fig. 5b as an example, the net production rate of CO is positive (produced) for $c < 0.75$, while it is negative (consumed) for $c > 0.75$, and thus CO concentration reaches maximum at $c = 0.75$. Thus, increasing the total reactivity will enhance CO production when c < 0.75, while enhance CO consumption when c > 0.75. Therefore, the sensitivity direction changes sign at local maximum concentration. The kinetic similarity is much weaker for the mass fraction of H radical compared to the temperature, and the less pronounced similarity could be attributed to the diffusion process [20]. While the diffusion process make the global similarity of all species less pronounced comparing with the homogenous ignition system in [20], the effect of diffusion on H radical is more significant comparing to CH_4 and CO, since H radical is one of the most important chain carriers and its diffusion is more pronounced due to the lighter molecular weight.

Similar independence of the strain rate has been previously observed in the sensitivity directions of OH concentration in the simulation of a turbulent lifted flame [5]. Therefore, the independence suggests that the sensitivity direction of ESR might be able to represent the sensitivity direction of the entire temperature field for turbulent premixed flames although a wide range of strain rates or scalar dissipation rates are involved in the flow field. Such representation could substantially accelerate the uncertainty quantification of turbulent combustion simulations as demonstrated in [1].

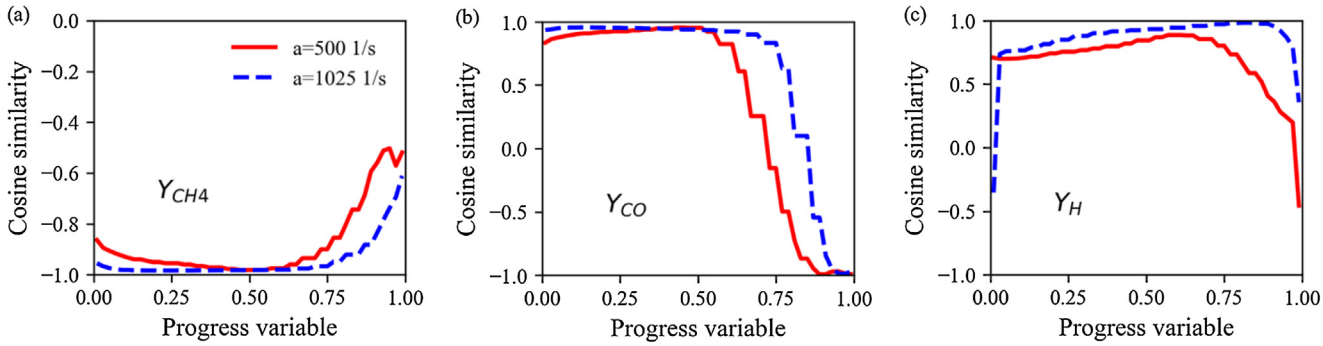

Fig. 5. The evolution of the sensitivity direction of species concentrations with the progress variable and strain rate. The cosine similarity is computed with respect to the sensitivity direction of ESR.

Finally, we briefly discuss how the universal sensitivity direction enables us to parameterize the uncertainties of hundreds of rate constants into one random variable, which is one of the key algorithms in [1]. Without loss of generality, let us assume that there are two rate constants, k_1 and k_2, in the chemical model. Perturbing them by Δ_1 and Δ_2, respectively, we can obtain three flamelet profiles including the unperturbed one, as shown in Fig. 3a. By definition, the temperature changes at two distinct locations x_1 and x_2 can be calculated with the corresponding sensitivity coefficients $[s_{1,1},\ s_{2,1}]$ and $[s_{1,2},\ s_{2,2}]$, and further related to the sensitivity directions $[\widetilde{s_{1,1}},\ \widetilde{s_{2,1}}]$, $[\widetilde{s_{1,2}},\ \widetilde{s_{2,2}}]$, as shown in Eqs. (4) and (5). Since there is a universal sensitivity direction across all locations, i.e., $[\widetilde{s_{1,1}},\ \widetilde{s_{2,1}}] = [\widetilde{s_{1,2}},\ \widetilde{s_{2,2}}]$, we can then parameterize the high-dimensional kinetic uncertainty as a single random variable ξ, according to Eq. (6). Therefore, the temperature response at any location due to the perturbation is always proportional to ξ, as shown in Eqs. (7) and (8), with the difference in the sensitivity magnitude. Similarly, since the universal sensitivity direction is also valid for various strain rates, the temperature response at any strain rate is also always proportional to ξ.

$$\Delta T(x_1) = s_{1,1}\Delta_1 + s_{2,1}\Delta_2 = \sqrt{s_{1,1}^2 + s_{2,1}^2}(\widetilde{s_{1,1}}\Delta_1 + \widetilde{s_{2,1}}\Delta_2) \tag{4}$$

$$\Delta T(x_2) = s_{1,2}\Delta_1 + s_{2,2}\Delta_2 = \sqrt{s_{1,2}^2 + s_{2,2}^2}(\widetilde{s_{1,2}}\Delta_1 + \widetilde{s_{2,2}}\Delta_2) \tag{5}$$

$$\xi = \widetilde{s_{1,1}}\Delta_1 + \widetilde{s_{2,1}}\Delta_2 = \widetilde{s_{1,2}}\Delta_1 + \widetilde{s_{2,2}}\Delta_2 \tag{6}$$

$$\Delta T(x_1) = \sqrt{s_{1,1}^2 + s_{2,1}^2}\ \xi \tag{7}$$

$$\Delta T(x_2) = \sqrt{s_{1,2}^2 + s_{2,2}^2}\ \xi \tag{8}$$

In the context of flamelet-based turbulent combustion simulations, the turbulent flames can be represented as ensembles of laminar flames under various strain rates. Since the sensitivity directions is independent of strain rate, one can imply that the entire turbulent flame also has a universal sensitivity direction. The magnitude of the sensitivity at different locations can be efficiently computed by sampling along the one-dimensional random variable ξ. It has been demonstrated that the uncertainties of the 325 reaction rate constants in the GRI 3.0 model were quantified with only 7 independent simulations with the rate constants varying along ξ [1]. Without assuming the universal sensitivity direction, direct Monte Carlo sampling would require at least 2000 samples [1].

The universal sensitivity direction could significantly expedite the uncertainty quantification of turbulent flame simulations if there are low-dimensional manifolds in turbulent premixed flames, such that we can use laminar flamelets to estimate the sensitivity direction. While such assumption is usually valid in the wrinkled and corrugated flamelet regimes, it is an open question whether the analysis still holds in the thin reaction zone and the broken reaction zone. We hope that current analysis can facilitate the research on uncertainty quantification of turbulent flames and provide an analysis framework to the community for future investigations.

4. Conclusions

We have shown that the kinetic sensitivity direction of extinction strain rate is similar to that of laminar flame speed for various kinds of fuels, equivalence ratios, and pressures. The similarity is consistent with the flame time scale analysis which shows that flame extinction and propagation share similar chemical time scale although the flame temperature at extinction is much lower. Furthermore, it is shown that the sensitivity direction of flame profiles is largely independent of the strain rates and progress variable. Moreover, the sensitivity directions of temperature and species concentrations are similar to that of extinction strain rate. The behavior could be attributed to the fact that the controlling reactions that determine the sensitivities of temperature are not altered by the maximum flame temperature. Therefore, the identified independence of sensitivity direction on strain rates and progress variable suggest that there exists a universal sensitivity direction in complex turbulent premixed flames involving a wide range of strain rates and progress variables. Furthermore, the direction can be estimated as the sensitivity directions of extinction strain rate and laminar flame speed. While the current study focuses on laminar premixed flames, the analysis framework can be extended to nonpremixed flames. These findings shall facilitate future algorithm development for sensitivity analysis and uncertainty quantification of turbulent combustion simulations.

Declaration of Competing Interest

The authors declare that they have no known competing financial interests or personal relationships that could have appeared to influence the work reported in this paper.

Acknowledgments

SD would like to acknowledge the support from the d'Arbeloff Career Development allowance at Massachusetts Institute of Technology. TY and ZR were supported by the National Natural Science Foundation of China 91841302.

References

[1] M.E. Mueller, G. Iaccarino, H. Pitsch, Chemical kinetic uncertainty quantification for Large Eddy Simulation of turbulent nonpremixed combustion, Proc. Combust. Inst. 34 (1) (2013) 1299–1306.

[2] H. Wang, D.A. Sheen, Combustion kinetic model uncertainty quantification, propagation and minimization, Prog. Energy Combust. Sci. 47 (2015) 1–31.

[3] W. Ji, Z. Ren, Y. Marzouk, C.K. Law, Quantifying kinetic uncertainty in turbulent combustion simulations using active subspaces, Proc. Combust. Inst. 37 (2) (2019) 2175–2182.

[4] X. Zhao, Y. Tao, T. Lu, H. Wang, Sensitivities of direct numerical simulations to chemical kinetic uncertainties: Spherical flame kernel evolution of a real jet fuel, Combust. Flame 209 (2019) 117–132.

[5] Z. Ren, S.B. Pope, Sensitivity calculations in PDF modelling of turbulent flames, Proc. Combust. Inst. 32 (1) (2009) 1629–1637.

[6] Z. Ren, S.B. Pope, Sensitivity calculations in PDF particle methods, Combust. Flame 153 (1–2) (2008) 202–215.

[7] K. Braman, T.A. Oliver, V. Raman, Adjoint-based sensitivity analysis of flames, Combust. Theory Model. 19 (1) (2015) 29–56.

[8] S.G. Davis, A.B. Mhadeshwar, D.G. Vlachos, H. Wang, A new approach to response surface development for detailed gas-phase and surface reaction kinetic model optimization, Int. J. Chem. Kinet. 36 (2) (2003) 94–106.

[9] C.K. Law, Combustion physics, Cambridge University Press, Cambridge, 2006.

[10] F.N. Egolfopoulos, P.E. Dimotakis, Non-premixed hydrocarbon ignition at high strain rates, Symp. Combust. 27 (1) (1998) 641–648.

[11] A.E. Long, R.L. Speth, W.H. Green, Ember: an open-source, transient solver for 1D reacting flow using large kinetic models, applied to strained extinction, Combust. Flame 195 (2018) 105–116.

[12] Y. Dong, A.T. Holley, M.G. Andac, F.N. Egolfopoulos, S.G. Davis, P. Middha, H. Wang, Extinction of premixed H_2/air flames: chemical kinetics and molecular diffusion effects, Combust. Flame 142 (4) (2005) 374–387.

[13] R.J. Kee, J.A. Miller, H. Jefferson, T Chemkin, A general-purpose, problem-independent, transportable, fortran chemical kinetics code package, Sandia Labs, 1980.

[14] H. Hashemi, J.G. Jacobsen, C.T. Rasmussen, J.M. Christensen, P. Glarborg, S. Gersen, M. van Essen, H.B. Levinsky, S.J. Klippenstein, High-pressure oxidation of ethane, Combust. Flame 182 (2017) 150–166.

[15] A.E. Long, R.L. Speth, W.H. Green, Numerical investigation of strained extinction at engine-relevant pressures: pressure dependence and sensitivity to chemical and physical parameters for methane-based flames, Combust. Flame 202 (2019) 318–333.

[16] C. Ji, E. Dames, Y.L. Wang, H. Wang, F.N. Egolfopoulos, Propagation and extinction of premixed C_5-C_{12} *n*-alkane flames, Combust. Flame 157 (2) (2010) 277–287.

[17] C. Ji, E. Dames, H. Wang, F.N. Egolfopoulos, Propagation and extinction of benzene and alkylated benzene flames, Combust. Flame 159 (3) (2012) 1070–1081.

[18] F.N. Egolfopoulos, C.K. Law, Chain mechanisms in the overall reaction orders in laminar flame propagation, Combust. Flame 80 (1) (1990) 7–16.

[19] E.S. Cho, S.H. Chung, T.K. Oh, Local karlovitz numbers at extinction for various fuels in counterflow premixed flames, Combust. Sci. Technol. 178 (9) (2006) 1559–1584.

[20] I.G. Zsély, J. Zádor, T. Turányi, Similarity of sensitivity functions of reaction kinetic models, J. Phys. Chem. A 107 (13) (2003) 2216–2238.

[21] J. Zádor, I.G. Zsély, T. Turányi, M. Ratto, S. Tarantola, A. Saltelli, Local and global uncertainty analyses of a methane flame model, J. Phys. Chem. A 109 (43) (2005) 9795–9807.

[22] I.G. Zsély, J. Zádor, T. Turányi, On the similarity of the sensitivity functions of methane combustion models, Combust. Theory Model. 9 (4) (2005) 721–738.

[23] W. Ji, Z. Ren, C.K. Law, Evolution of sensitivity directions during autoignition, Proc. Combust. Inst. 37 (1) (2019) 807–815.

[24] K. Kumar, C.J. Sung, Laminar flame speeds and extinction limits of preheated *n*-decane/O_2/N_2 and *n*-dodecane/O_2/N_2 mixtures, Combust. Flame 151 (1–2) (2007) 209–224.

[25] S.M. Sarathy, M.J. Thomson, C. Togbé, P. Dagaut, F. Halter, C. Mounaim-Rousselle, An experimental and kinetic modeling study of *n*-butanol combustion, Combust. Flame 156 (4) (2009) 852–864.

[26] P.S. Veloo, Y.L. Wang, F.N. Egolfopoulos, C.K. Westbrook, A comparative experimental and computational study of methanol, ethanol, and *n*-butanol flames, Combust. Flame 157 (10) (2010) 1989–2004.

[27] A.T. Holley, Y. Dong, M.G. Andac, F.N. Egolfopoulos, Extinction of premixed flames of practical liquid fuels: experiments and simulations, Combust. Flame 144 (3) (2006) 448–460.

[28] Y.L. Wang, A.T. Holley, C. Ji, F.N. Egolfopoulos, T.T. Tsotsis, H.J. Curran, Propagation and extinction of premixed dimethyl-ether/air flames, Proc. Combust. Inst 32 (1) (2009) 1035–1042.

[29] K. Kumar, C.-J. Sung, Flame propagation and extinction characteristics of neat surrogate fuel components, Energy Fuels 24 (7) (2010) 3840–3849.

[30] Y.L. Wang, Q. Feng, F.N. Egolfopoulos, T.T. Tsotsis, Studies of C_4 and C_{10} methyl ester flames, Combust. Flame 158 (8) (2011) 1507–1519.

[31] X. Hui, A.K. Das, K. Kumar, C.J. Sung, S. Dooley, F.L. Dryer, Laminar flame speeds and extinction stretch rates of selected aromatic hydrocarbons, Fuel 97 (2012) 695–702.

[32] W. Xu, Y. Jiang, R. Qiu, X. Ren, Influence of halon replacements on laminar flame speeds and extinction limits of hydrocarbon flames, Combust. Flame 182 (2017) 1–13.

[33] N. Peters, Length scales in laminar and turbulent flames, Numerical Approaches to Combustible Modelling, 135, American Institute of Aeronautics and Astronautics, Washington DC (1991), pp. 155–182.

[34] B. Rogg, Response and flamelet structure of stretched premixed methane/air flames, Combust. Flame 73 (1) (1988) 45–65.

[35] W. Ji, J. Wang, O. Zahm, Y.M. Marzouk, B. Yang, Z. Ren, C.K. Law, Shared low-dimensional subspaces for propagating kinetic uncertainty to multiple outputs, Combust. Flame 190 (2018) 146–157.

[36] G.P. Smith, D.M. Golden, M. Frenklach, N.W. Moriarty, B. Eiteneer, M. Goldenberg, C.T. Bowman, R.K. Hanson, S. Song, W.C. Gardiner Jr, GRI 3.0 Mechanism. available at <www.me.berkeley.edu/gri_mech>.